# IRREGULAR COMPONENT OF IONOSPHERIC REFRACTION

Terence J. Elkins

Air Force Cambridge Research Laboratories
L. G. Hanscom Field, Massachusetts

1970

UNCLASSIFIED

SECURITY CLASSIFICATION OF THIS PAGE (When Data Entered)

# REPORT DOCUMENTATION PAGE

READ INSTRUCTIONS BEFORE COMPLETING FORM

| | |
|---|---|
| 1. REPORT NUMBER: AFCRL-TR-74-0431 | 2. GOVT ACCESSION NO. |
| 3. RECIPIENT'S CATALOG NUMBER | |
| 4. TITLE (and Subtitle): Irregular Component of Ionospheric Refraction | 5. TYPE OF REPORT & PERIOD COVERED: Scientific. Interim. |
| 6. PERFORMING ORG. REPORT NUMBER | |
| 7. AUTHOR(s): Terence J. Elkins | 8. CONTRACT OR GRANT NUMBER(s) |
| 9. PERFORMING ORGANIZATION NAME AND ADDRESS: Air Force Cambridge Research Laboratories, Hanscom AFB, MA 01730, Ionospheric Physics Laboratory | 10. PROGRAM ELEMENT, PROJECT, TASK AREA & WORK UNIT NUMBERS: 62101F 681300 P46430101 |
| 11. CONTROLLING OFFICE NAME AND ADDRESS: Air Force Cambridge Research Laboratories, Hanscom AFB, MA 01730 | 12. REPORT DATE: 5 February 1971 |
| | 13. NUMBER OF PAGES: 24 pages |
| 14. MONITORING AGENCY NAME & ADDRESS (if different from Controlling Office) | 15. SECURITY CLASS. (of this report): Unclassified |
| | 15a. DECLASSIFICATION/DOWNGRADING SCHEDULE |

16. DISTRIBUTION STATEMENT (of this Report)

Approved for public release; distribution unlimited.



17. DISTRIBUTION STATEMENT (of the abstract entered in Block 20, if different from Report)

18. SUPPLEMENTARY NOTES

Reprinted from Ionospheric and Tropospheric Limitations to Radar Accuracy (AFCRL-71-0169)

19. KEY WORDS (Continue on reverse side if necessary and identify by block number)

Ionospheric Irregularities
Radar Refraction

20. ABSTRACT (Continue on reverse side if necessary and identify by block number)

The effect of small to medium scale ionospheric irregularities on the pointing accuracy of UHF radars is examined for mid- and high-latitude sites. Refraction and range errors are estimated for typical situations as well as their elevation dependence. Examples of specific radar locations are presented.



DD FORM 1 JAN 73 1473 EDITION OF 1 NOV 65 IS OBSOLETE

UNCLASSIFIED

SECURITY CLASSIFICATION OF THIS PAGE (When Data Entered)

Contents



# 5. Irregular Component of Ionospheric Refraction

T.J. Elkins
Ionospheric Physics Laboratory

## 5.1 INTRODUCTION

For the purposes of this report, ionospheric irregularities which contribute to the variable component of refraction will be considered in two categories, determined principally by the time scale on which their effects are manifested: (1) A large scale component, due to travelling disturbances, or waves moving through the ionosphere, having periods in the range ~15-100 minutes, (2) Rapid angle "jitter", with a time scale (for a stationary target) from several seconds to several tens of seconds, caused by irregularities having a characteristic dimension of the order of one kilometer.

From the viewpoint of an operational radar, the large irregularities would cause an apparent bias error which varies slowly throughout a "pass". The angular errors due to small irregularities could be reduced by integration over a relatively small section of the target trajectory (several kilometers). A very slowly varying component due to changing solar illumination as the earth rotates and as the seasons progress, will not be considered in this section.

There have been relatively few experimental studies of irregular ionospheric refraction, especially in the high-latitude region where the incidence of ionospheric irregularities is far greater than at midlatitudes. It is possible to form

some estimates for "typical" or "average" conditions, but the extremely variable and disturbed nature of the high-latitude ionosphere makes it necessary to use these estimates with caution. The situation at midlatitudes is moderately well understood, and can be specified with some degree of confidence.

This section will deal principally with observations of irregular ionospheric refraction, both at AFCRL and elsewhere, supplemented where necessary by theoretical and numerical estimates. Although it is possible, at least in principle, to use three-dimensional, ray-tracing programs to compute the refraction through arbitrary electron-density distributions, there does not yet exist sufficiently detailed knowledge of these distributions to make this approach worthwhile.

## 5.2 FREQUENCY AND ALTITUDE SCALING LAWS

Various observers have measured ionospheric refraction at a variety of radio frequencies. In order to reduce all available observations to the actual radar frequencies, it is necessary to establish a frequency scaling law. At frequencies well in excess of the maximum plasma frequency in the ionosphere, the refraction angle varies inversely as the square of the radio frequency (Bailey, 1948). This theoretical prediction is amply borne out by ray-tracing studies (Pfister and Keneshea, 1956; Millman, 1967; and Weisbrod and Colin, 1960) Many of the observations of irregular refraction have used radio stars or geostationary satellites, at ranges which are essentially infinite, so that the quantity being measured is actually astronomical refraction. This differs, of course, from the ray bending for a target within the dispersive medium (the ionosphere). For targets at ionospheric altitudes, it is necessary to apply corrections when using astronomical refraction data for comparison purposes. This may be accomplished, to a reasonable degree of accuracy, by applying a weighting factor, computed by tracing rays through a typical ionospheric profile. This weighting factor is a function of target altitude, and it may be estimated from Figure 5.1 which makes use of the results of Carru et al (1960) with suitable frequency scaling factors applied. Each individual curve normalizes the angular deviation to the astronomical refraction for that elevation angle.

## 5.3 LARGE SCALE COMPONENT OF IRREGULAR REFRACTION

The ionosphere departs from its idealized quiescent condition of horizontal stratification when perturbed by the passage of an atmospheric wave. At midlatitudes (that is, less than $\sim 60^{\circ}$), these waves have the character of ripples or wrinkles in the ionosphere, with fronts extending over several thousand kilometers.

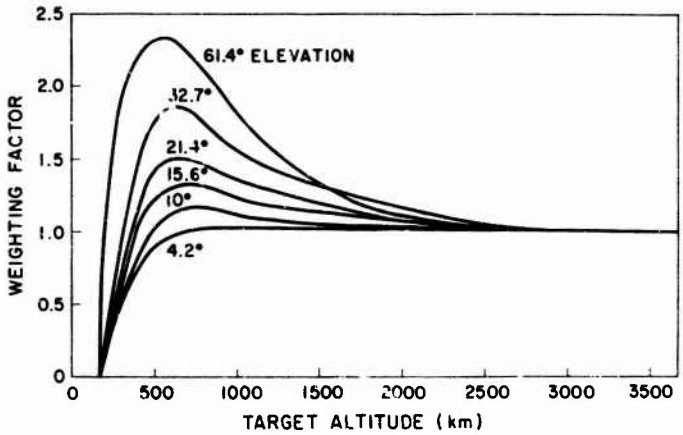


Figure 5.1. Weighting Factor for Converting Astronomical Refraction to Angular Deviation at Target Altitude for Various Elevation Angles

The altitude of any given contour of constant electron density may vary by 100 km or more, and the columnar electron content may vary by several percent of the mean total content (probably considerably greater at high latitudes). Such events are found to have wavelengths of ~50-1000 km, and very often to travel towards the equator from the auroral zones. They have predictable diurnal and seasonal variations for midlatitude locations.

## 5.4 ANGLE JITTER

The effect of small-scale irregular structure of the F-region is to introduce diffraction phase structure into the radio wavefronts emerging from the disturbed ionospheric region. At frequencies in the UHF range, this may be equivalent to angular "noise" of the order of one to one tenth milliradians. The variance of this phase noise, or "flicker" may be expressed as

$$\overline{\theta^2} = 2\overline{\phi^2}\left(\frac{\lambda}{2\pi d}\right)^2 \qquad (5.1)$$

where

- $\theta$ is the instantaneous angular deviation
- $\lambda$ is the radio wavelength
- d is the characteristic (dominant) irregularity size
- $\phi$ is the instantaneous phase deviation, over distance d along the wavefront.

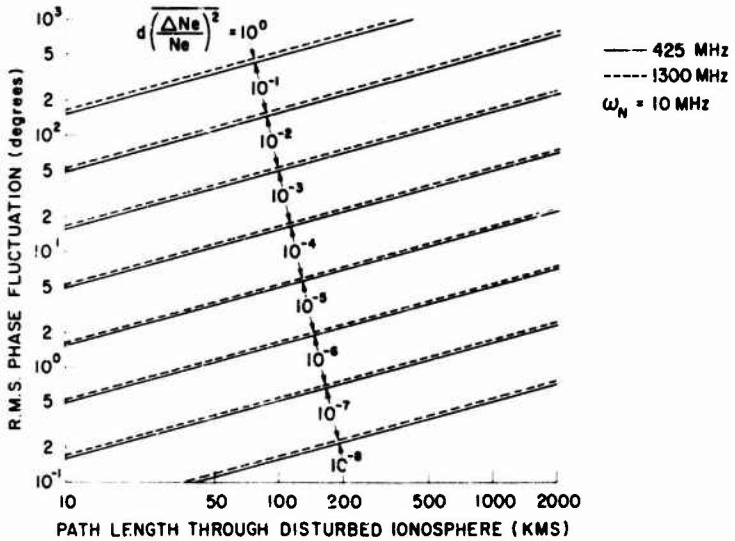


Figure 5.2. Variation of RMS Phase Perturbation With Length of Ray Path Through the Disturbed Ionosphere, at 425 MHz and 1300 MHz. Computations are for a plasma frequency of 10 MHz and for various mean square electron density perturbations

The bar denotes time averaging. The irregularity dimension is typically several hundred meters, and $\overline{\phi^2}$ is related to the intensity of the electron density perturbations. It has been shown in Booker (1958) that $\overline{\phi^2}$ may be expressed as

$$\overline{\phi^2} = \frac{d\,L\,\omega_n^4}{4c^2\omega^2}\left(\frac{\overline{\Delta N_e}}{N_e}\right)^2 \qquad (5.2)$$

where

L = path length through the irregularity region
c = velocity of light
$N_e$ = electron concentration
$\Delta N_e$ = electron density perturbation
$\omega_n$ = plasma frequency

Following the example of Millman (1967), the rms phase deviation has been plotted in Figure 5.2 using Eq. (5.2) for the two radar frequencies. Measurements of the electron-density perturbations have been reported by Dyson (1969) for auroral and high latitudes. These measurements, performed in situ by means of Langmuir probes mounted on board Alouette 2, indicate that the most common irregularity

thickness is 500-1000 meters, and that an appreciable proportion of irregularities have electron concentrations differing from the background by 50 per cent and more. As an illustration of the use of Figure 5.2, for a path length of 200 km through a region containing 10 percent irregularities of 1 km thickness, the phase deviation at 425 MHz would be 215 degrees, and 70 degrees at 1300 MHz. Such a phase deviation may be appropriate to an auroral zone location (Fairbanks).

## 5.5 SCINTILLATION MORPHOLOGY

There is little available data on rapid angular fluctuations, but a great deal of data have been accumulated in the study of ionospheric amplitude scintillation. The normalized variance of the amplitude scintillation is given by

$$\left(\frac{\overline{\Delta A}}{A}\right)^2 = \frac{Z^2 \lambda^2}{d^4} \overline{\phi^2} \qquad (5.3)$$

where

A is the instantaneous signal amplitude

z is the range of the irregularities

By studying the diurnal, seasonal and geographic variations of amplitude scintillation, it is possible to establish qualitatively these same parameters for angular fluctuation, even though the amplitude scintillation technique is less sensitive than a phase or angle scintillation technique. This approach will be used in this report in order to circumvent the lack of necessary angle fluctuation data for the various radar sites.

## 5.6 MIDLATITUDE SITES

The radar at Diyarbakir is located on an invariant L-shell (McIlwain, 1961) of 1.8, which means that the irregularity behavior at this location should be of characteristically midlatitude type. At midlatitudes, the principal irregularity structure is the travelling ionospheric disturbance (TID) or atmospheric wave, which is thought to propagate from some source located in the auroral zones (probably auroral sub-storms). These large scale disturbances give rise to horizontal gradients of electron density, which cause both elevation and azimuth refraction errors. The direction of the maximum gradient, and consequently the maximum refraction error, may be assumed to be in the magnetic meridian plane at the solstices, and approximately normal to this direction at the equinoxes, according to Munro (1958) and Jones (1969), reproduced in Figure 5.3. Measurements of the gradient of total electron content at midlatitudes have been reported

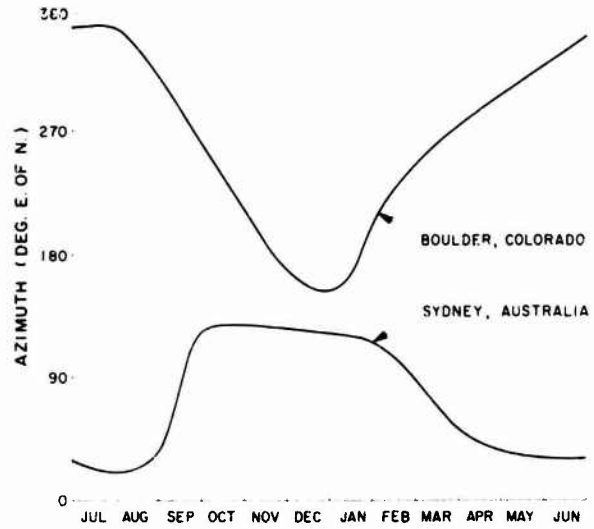


Figure 5.3. Seasonal Variation of Direction of Propagation of travelling Ionospheric Disturbances (TID), for Both Hemispheres (after Jones, (1969)

in the literature, for example, by Bhonsle (1966) and Titheridge (1968). In New Zealand, the observations of Titheridge (1968) indicate that a horizontal gradient of $2 \times 10^{10} m^{-3}$ may be a typical value for that area. Other observations in California (Bhonsle, 1966) using a more sensitive technique indicate a smaller average magnitude for horizontal gradients ($7 \times 10^{9} m^{-3}$). The percentage deviation from the ambient total electron content is virtually independent of the time of day, and varies approximately linearly with the spatial scale of the irregularity. These observations of horizontal electron content gradients may be reduced to zenith refraction errors by the following formula for wedge refraction (Lawrence et al, 1964):

$$\tau = \frac{b}{\omega^2} \nabla (TEC) \qquad (5.4)$$

where

$b = 1.6 \times 10^{3}$ mks units

$\tau$ = refraction angle

$\omega$ = angular frequency

TEC = total electron content

At 425 MHz, a horizontal gradient of $2 \times 10^{10} m^{-3}$ results in bending of a vertically incident ray by 0.005 mr.

Similarly, the group path delay, $\delta \ell$, may be estimated from (Lawrence et al, 1964):

$$\delta \ell = \frac{b}{\omega^2} \text{ (TEC)}. \tag{5.5}$$

Thus, for a typical total electron content of $5 \times 10^{17}$ $m^{-2}$, and for a 5 percent irregularity, the group path delay at 425 MHz is 5.7 meters. For a hypothetical stationary target, the horizontal motion of the irregularity itself would give an apparent range rate of $\sim 0.01$ m $sec^{-1}$, assuming a typical irregularity velocity of 150 m $sec^{-1}$. Actual range rates due to target motion would, of course, be much larger than this value.

The radar station of Shemya ($L \sim 2.4$) lies close to the transition zone between midlatitude and auroral regions, and thus presents some special problems. The level of ionospheric activity is quite variable in this region, and in general is considerably higher than for the lower latitude site. In particular, there may be a considerable difference between observations to the North and to the South during periods of moderate to high magnetic activity, since the ionosphere in these directions behaves, respectively, as a high latitude and midlatitude ionosphere. The situation is complicated by the fact that the location of this boundary region moves in the magnetic North-South direction as the level of magnetic activity varies. Another distinctive feature of the ionosphere in this region is the presence of the midlatitude ionization trough, which is a large depression of electron concentration aligned along the invariant shells $L = 3.5 \sim 4.0$. One may expect the greatest refraction errors due to the midlatitude trough when the radar is pointing at an azimuth tangent to the trough (that is, roughly North-East or North-West). A ray-tracing solution for the problem of propagation through the trough at 400 MHz has been reported in "The Millstone Hill Propagation Study" (1969). The refractive index model used in this study is reproduced in Figure 5.4, while the computed elevation and azimuth errors are reproduced in Figure 5.5 as a function of azimuth bearing, after subtracting the mean refraction.

The magnitude of the large scale irregularities can be estimated from long baseline interferometer observations performed at the Sagamore Hill Radio Observatory of AFCRL, located at $L = 3.5$. These observations used beacon transmissions at 137 MHz from geostationary satellites, and were measured with the interferometer situated in the local magnetic meridian plane. Figure 5.6 shows a typical frequency-scaled sample of data from this interferometer, with astronomical refraction in the meridian plane presented as a function of local time. For convenience in comparing diverse results, the magnitude of the variable refraction component has been reduced approximately to the equivalent value at the zenith, using a method which will be explained shortly. Notice that the largest refraction events take place at around midnight and local noon. The fluctuations near midnight are typically much more erratic and dependent upon magnetic activity than those occurring in the daytime. In contrast with daytime events, they are

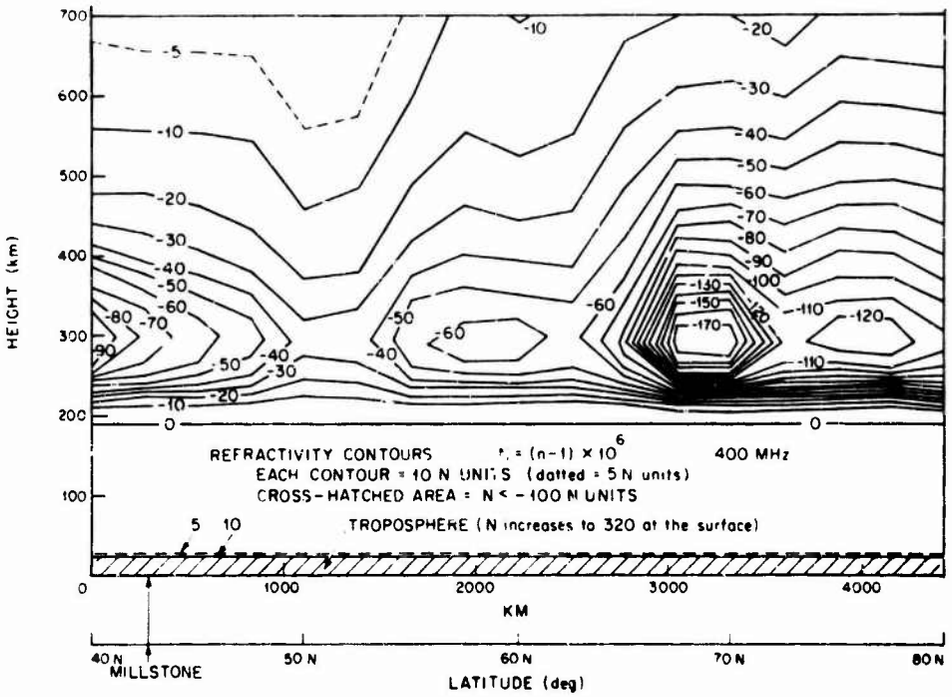


Figure 5.4. Contours of Refractive Index for Northern Midlatitudes, Showing the Midlatitude Trough (The Millstone Hill Propagation Study, 1969)

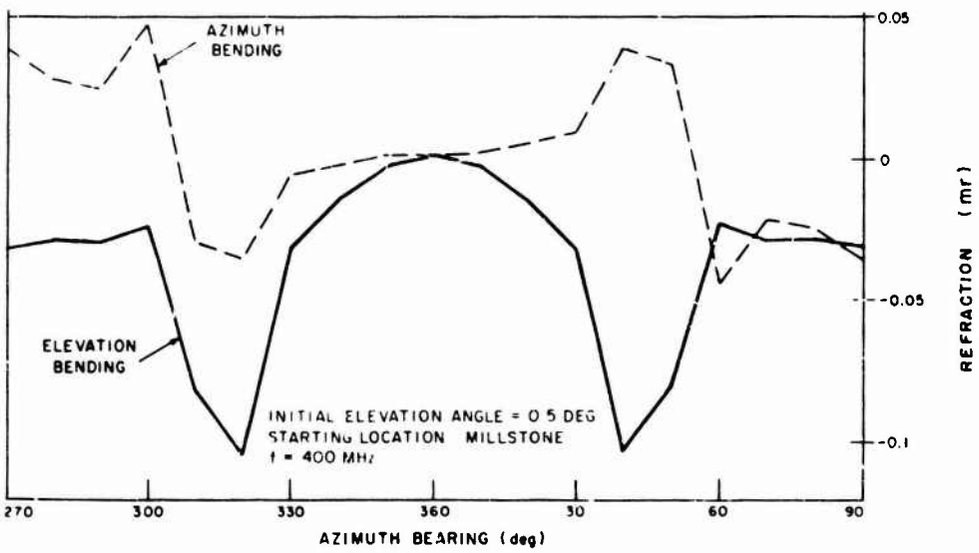


Figure 5.5. Elevation and Azimuth Components of Ray Bending at 400 MHz, Computed by Ray Tracing Through Refractive Index Profile of Figure 5.4, Starting at Millstone Hill. Mean Bending Has Been Subtracted (The Millstone Hill Propagation Study, 1969)

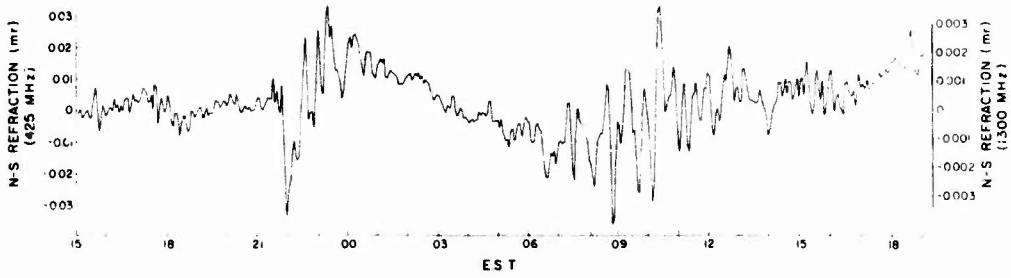


Figure 5.6. A Typical Sample of Data From the Long Baseline Interferometer at AFCRL, Showing Irregular Refraction, Scaled to Radar Frequencies, as a Function of Local Time. Refraction is reduced to zenith value

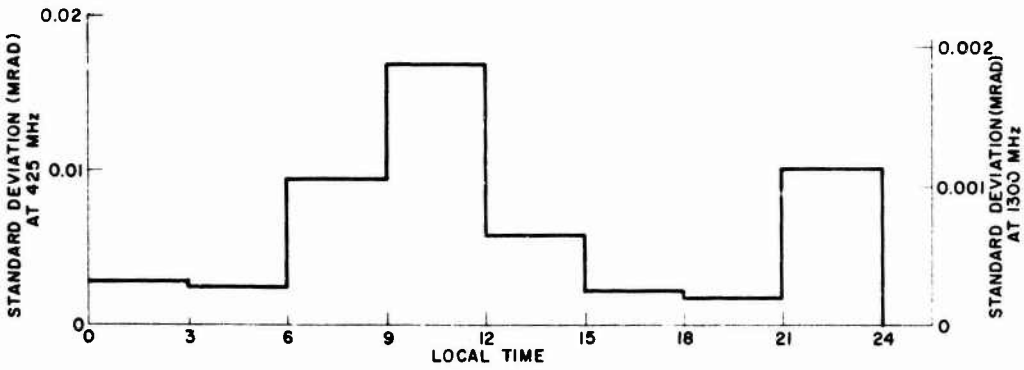


Figure 5.7. Histogram Showing Standard Deviation of the Irregular Component of Refraction in 3-hour Time Increments, for the Sample of Data Reproduced in Figure 5.6

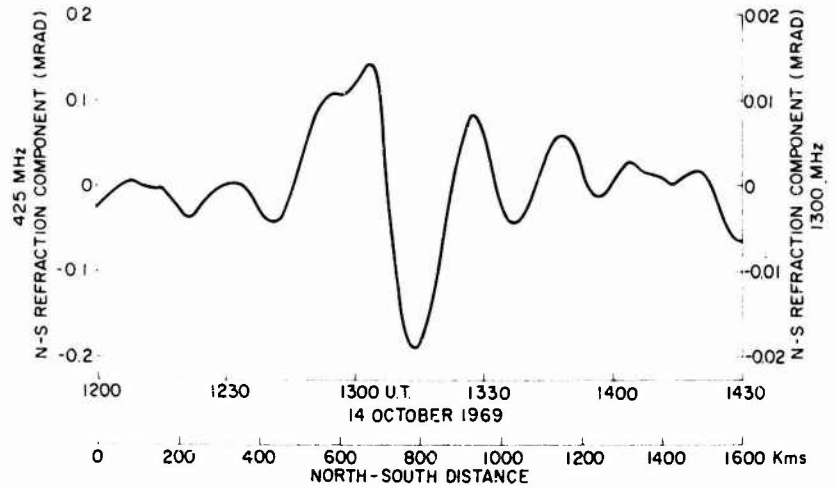


Figure 5.8. An Individual "Smooth" Refraction Event, Caused by a Train of Atmospheric Waves, Observed With AFCRL Interferometer. Magnetic North-South refraction component is shown, reduced to zenith refraction at 425 MHz and 1300 MHz, as a function of time and of horizontal distance in the ionosphere

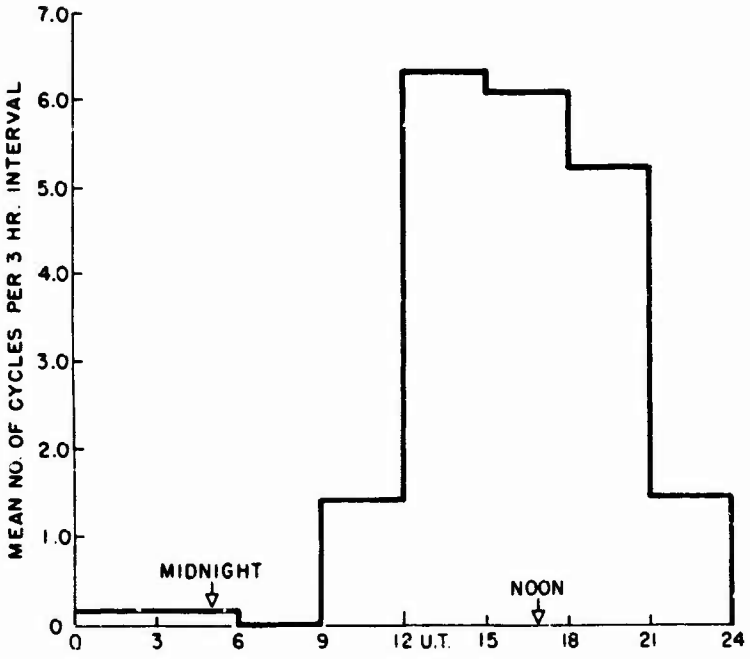


Figure 5.9. Histogram of the Diurnal Variation of "Smooth" Refraction Events, Such as That in Figure 5.8, Showing a Pronounced Maximum Shortly Before Local Noon

usually accompanied by strong amplitude and phase scintillations. For these reasons, daytime and nighttime events have been considered separately in this report, since they will present quite distinguishable observing conditions in practice.

Figure 5.7 shows the standard deviation of the irregular refraction for the sample reproduced in Figure 5.6, as a histogram in 3-hour time increments. Daytime refraction events are observed almost every day at Sagamore Hill, and have a distinctive smoothly varying character. Figure 5.8 shows an individual "smooth" refraction event - among the largest observed at Sagamore Hill. Other observations have established that the ionospheric motions producing such events have horizontal velocities of the order of 150 m $sec^{-1}$. Using this velocity, a horizontal distance scale has been added to Figure 5.8, in order to indicate how the refraction error might vary during target tracking over a large distance. Figure 5.9 shows the diurnal variation of "smooth" events for a typical month. Experience has shown that this diurnal variation is independent of season, but that the amplitude of the refraction events has a seasonal variation, being largest in winter and smallest in summer.

It has been observed that the refraction events at Sagamore Hill are usually associated with long fronts elongated in the East-West direction, and with maximum gradients in the North-South direction, which is the direction in which the refraction is measured. No data have been accumulated for the East-West refraction component. However, at a similar magnetic latitude, observations of radio stars at 81.5 MHz (Smith, 1952) indicated that a value of ± 0.006 mr might be observed at 425 MHz for East-West refraction, which is less than one third of the probable North-South component. The possibility that the direction of the elongated fronts may vary seasonally, as indicated in Figure 5.3, suggests that this asymmetry may not always be as simple as here indicated, but the simpler situation is probably more likely at Shemya than at Diyarbakir.

It is interesting to note that long baseline interferometer observations of radio astronomical sources at 2695 MHz at West Virginia, reported by Basart (1970) agree quite well with the above estimates when suitably scaled. On an 11.3 km baseline, rms differential phase changes were reported as follows:

Short term (minute to minute): $5^{o}$

Long term (10 - 45 minutes): $\sim 10^{o}$ - $30^{o}$

At 425 MHz, these measurements imply angular errors of 0.008 mr and 0.016 mr - 0.048 mr, respectively.

## 5.7 ANGULAR FLICKER AND MIDLATITUDES

Although angular flicker or scintillation is highly sporadic in nature, and virtually impossible to predict in any individual instance, its gross morphology is reasonably well understood for a midlatitude location. For a hypothetical stationary target, the instantaneous angular position appears to fluctuate on a time scale of several seconds to several tens of seconds, due to the motion of small ($\sim$ 1 km across) ionospheric irregularities across the ray path. However, it must be recalled that the fluctuation rate will be much more rapid for a target moving at a high velocity transverse to the radar. Whereas a typical velocity for ionospheric irregularity motion is 100-200 m $sec^{-1}$, a typical transverse target velocity may be 6 km $sec^{-1}$. Thus the targe flicker would be observed on a time scale of some tens to hundreds of milliseconds. Integration of instantaneous target position over periods of the order of one half second or less may, therefore, be expected to reduce target flicker substantially.

The magnitude of the angular fluctuations may be estimated from Eqs. (5.1) and (5.2), using suitable observational data, which is predominantly of amplitude fluctuations. Such observations, by many different workers have been

summarized, for example by Getmantsev and Eroukhimov (1969), where it is apparent that a figure of ~ 1 km is most commonly found for the thickness of individual irregularities, and an rms electron-density perturbation of $\sim 10^{-3}$ or less is appropriate for midlatitudes. These small irregularities are distributed over an altitude range of 100 km to more than 1000 km, but are not uniformly distributed, as often assumed in theoretical calculations; rather, they are observed to occur in patches with vertical extent ~ 100 km, and with horizontal dimensions of some hundreds of kilometers. From these data, the rms angular fluctuation at midlatitudes, under conditions of moderate magnetic activity may be estimated at 0.005 mr, for a frequency of 425 MHz, and 0.0005 at 1300 MHz. A typical value under disturbed ionospheric conditions may be an order of magnitude larger than these figures. These estimates are supported by measurements of the phase scintillation pattern using the Sagamore Hill interferometer. During disturbed conditions, for example at 137 MHz, the rms phase perturbation is observed to be ~ 0.5 - 1.0 radians, which when scaled to the radar frequencies, yields estimates of angular flicker in fair agreement with the figures quoted above. Very few actual measurements of angular scintillation have been reported. For comparison, extrapolating the results of Hewish (1952) and Lawrence et al (1961) to 425 MHz yields values of 0.006 to 0.009 mr for quiet periods, and 0.032 to 0.077 mr for disturbed periods.

## 5.8 MORPHOLOGY OF ANGULAR FLICKER AT MIDLATITUDES

Figure 5.10 shows the diurnal variation of amplitude fading occurrence at 137 MHz for a geostationary satellite observed from Cold Bay, Alaska (55.3°N; 162.8°W). This diurnal variation may be taken to be the same as that for the Shemya site, which is relatively close to Cold Bay. On this basis, the maximum incidence of angular flicker may be expected at around local midnight. Figure 5.11 shows the diurnal variation of amplitude scintillation index for observations of two geostationary satellites at 137 MHz from Sagamore Hill, showing that the intensity of scintillation maximizes near midnight, as well as the frequency of occurrence, as indicated in Figure 5.10. The small difference between the peaks of the two curves in Figure 5.11 is due to the small longitude difference between the ionospheric intersection points of the ray paths to the two satellites. Figure 5.12 shows the seasonal variation in incidence of amplitude scintillation at Cold Bay, for the only available 6-month period. In summer, observable scintillation occurred on almost every night, whereas in winter, amplitude scintillation was only about one fourth as prevalent.

Irregular angular scintillation is expected less frequently at the Diyarbakir site than at Shemya, and the diurnal pattern is somewhat different. Figure 5.13 shows the diurnal variation of scintillation occurrence at Haifa (35° E; 32.8° N)

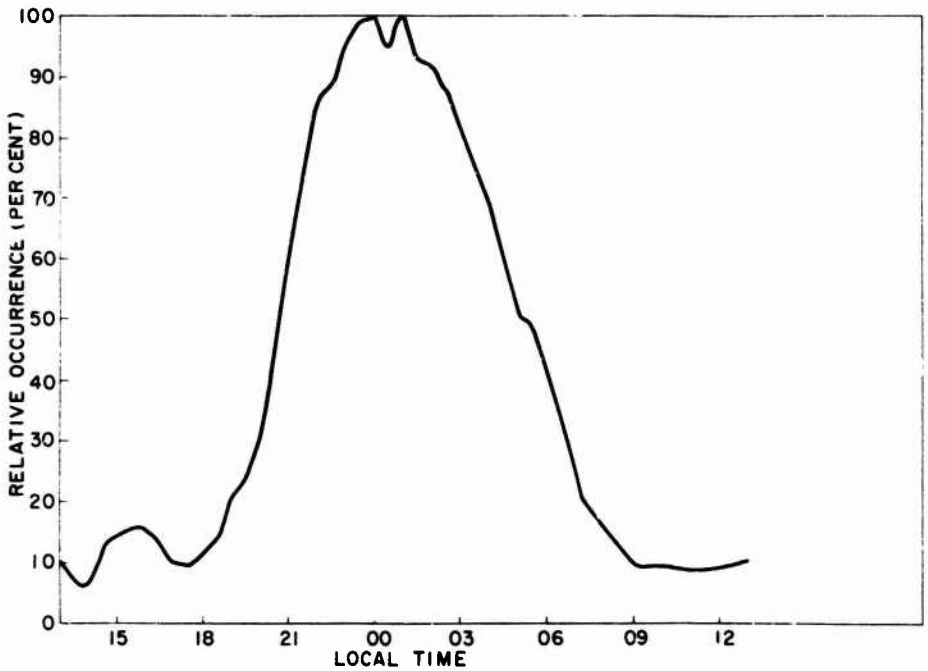


Figure 5.10. Diurnal Variation of Occurrence of Amplitude Scintillation of a Geostationary Satellite Beacon at Cold Bay, Alaska (55.3°N; 162.8°W), Which is Representative of Conditions at Shemya

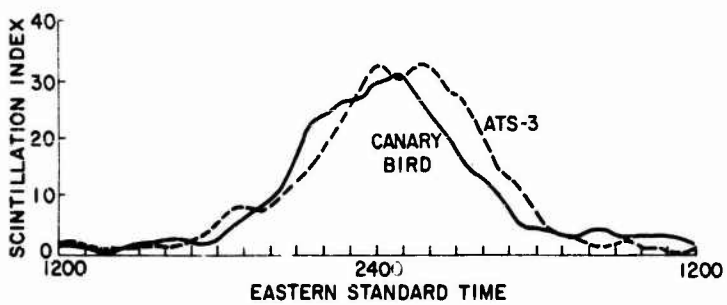


Figure 5.11. Diurnal Variation of Amplitude Scintillation Index at Sagamore Hill (L=3.5) for Two Geostationary Satellite Beacons at 137 MHz. Small time difference between the two maxima is due to the longitude separation of the ionospheric intersections of the two ray paths

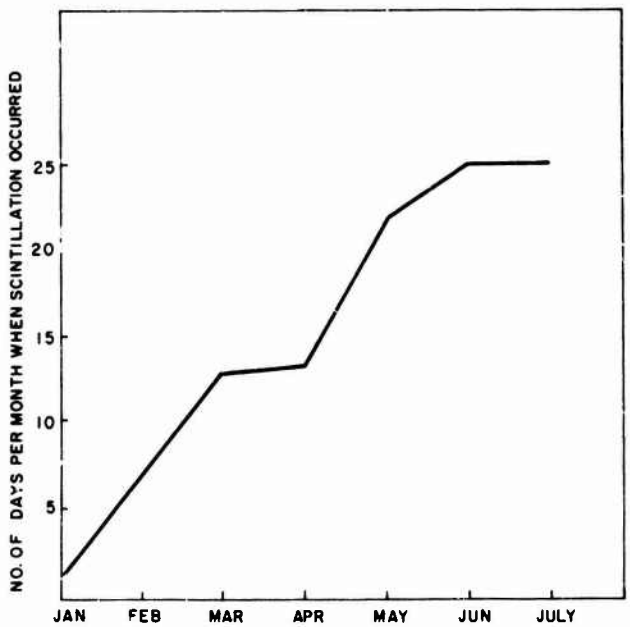


Figure 5.12. Seasonal Variation of Occurrence of Amplitude Scintillation at Cold Bay, Alaska for a Six Month Recording Period

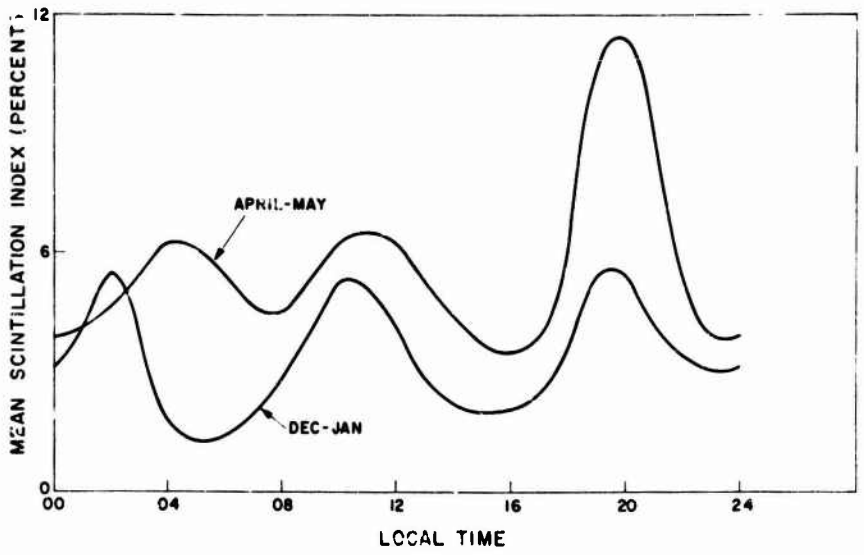


Figure 5.13. Diurnal Variation of Occurrence of Amplitude Scintillation at Haifa (32.8°N; 35°E), Which is Representative of Conditions at Diyarbakir (Houminer, 1969)

which is reasonably close to Diyarbakir (Houminer, 1969). There are three peaks at roughly 8-hour intervals, with no unusual effects near midnight, as expected at Shemya.

## 5.9 HIGH LATITUDE SITES

The radars at Clear, Alaska and at Thule, Greenland may be classified as high latitude locations, from the point of view of ionospheric irregularity. Nevertheless, there is a considerable difference between the irregular properties of the ionosphere at these two locations, which derives basically from the complex phenomena associated with the interaction between the earth's magnetosphere and the high latitude ionosphere. The radar at Clear is located in the zone of maximum auroral activity, which is the most disturbed and variable region of the ionosphere. The dominant feature of the ionosphere in this zone is the association of all forms of irregular ionospheric behavior with visible and subvisual aurora. For example, in the present connection, observations have been reported (Fremouw, 1967) of angular tracking errors of satellites at 136 MHz of several degrees, when the radar was pointing near active aurora. When scaled to 425 MHz, this would indicate possible errors of ~5 mr, or two orders of magnitude greater than typical midlatitude errors.

Active aurora is less common at Thule than at Clear, but the general level of ionospheric irregularity inside the polar cap is higher even than the auroral zone. The biggest problem in specifying the expected angular errors in this region is the lack of available information, since very few experimental studies have been conducted in the polar cap region. The estimates of refraction error and morphology will be correspondingly less reliable than for the midlatitude sites. The polar ionosphere is so disturbed that its most characteristic feature is its irregular properties. Chapter 4 of this report, devoted entirely to the polar ionosphere, contains a more thorough treatment of this subject.

## 5.10 LARGE SCALE IRREGULARITIES AT HIGH LATITUDES

It was noted by Mityakov et al (1968) that the smoothly varying, quasi-sinusoidal disturbance observed at midlatitudes are not observed to the North of 64° geomagnetic latitude. However, very large irregular horizontal gradients of total electron content are observed. Radio star observations with interferometers at Fairbanks, Alaska (Fremouw and Lansinger, 1968) have shown that weak auroral forms can cause refraction errors of 36.3 and 23.5 minutes of arc at 68 MHz, in two specific cases. These errors would be associated with horizontal gradients

of $\sim 0.8 - 1.2 \times 10^{12}$ m$^{-3}$, and are equivalent to refraction errors of 0.27 mr and 0.17 mr, respectively, at 425 MHz. While an order of magnitude larger than midlatitude errors, these figures are still an order of magnitude less than the errors reported in (Fremouw and Lansinger, 1968) for active aurora, thus indicating the extreme variability of the auroral ionosphere. Few measurements are available, inside the polar cap, of large scale irregularities. Stuart and Titheridge (1969) reported mean horizontal gradients of $2 \times 10^{10}$ m$^{-3}$, which value exhibited little diurnal variation, in contrast with the situation for small scale irregularities. A horizontal gradient of this order is typical for a midlatitude location. However the data in the study cited have been averaged over an interval of 2 hours. Since it is known (see Section 4.6) that large scale irregularities vary much more rapidly than this, it seems certain that this averaging procedure has severely underestimated the instantaneous magnitude of large irregularities inside the polar cap.

While visual aurora is relatively uncommon at Thule, it may on occasion cause noticeable effects. The so called "auroral oval" represents the zone of maximum occurrence of visual aurora, and approximates closely the ionospheric termination of the boundary between open and closed magnetic-field lines in the magnetosphere. The oval is located at geomagnetic latitudes of 69° - 75° near midnight, and at 80° - 85° near local noon. Thus, a radar looking South from Thule may encounter visual aurora with consequent large refraction errors similar to those more commonly observed at Clear during the night. However, aurora at Thule is generally of low luminosity, associated with low-energy incident particles, so that the refraction errors may be similar to those observed during weak aurora at Clear.

## 5.11 SMALL SCALE IRREGULARITIES AT HIGH LATITUDES

The most comprehensive study of small scale irregularities at high latitudes (Stuart and Titheridge, 1969) may be partially summarized as follows:

(1) For regions within the polar cap (for example, Thule) the degree of irregularity has a pronounced diurnal variation which maximizes at 2200 local time in summer, and at 1900 local time in winter. This diurnal dependence is observed during all phases of the solar cycle.

(2) Outside the polar cap region (for example, Clear) the diurnal variation is such that maximum irregularity occurs at around 1900 local time, with a minimum near local noon. This diurnal variation is most pronounced at the equinoxes and at sunspot maximum. At sunspot minimum there is little or no diurnal variation in irregularity incidence.

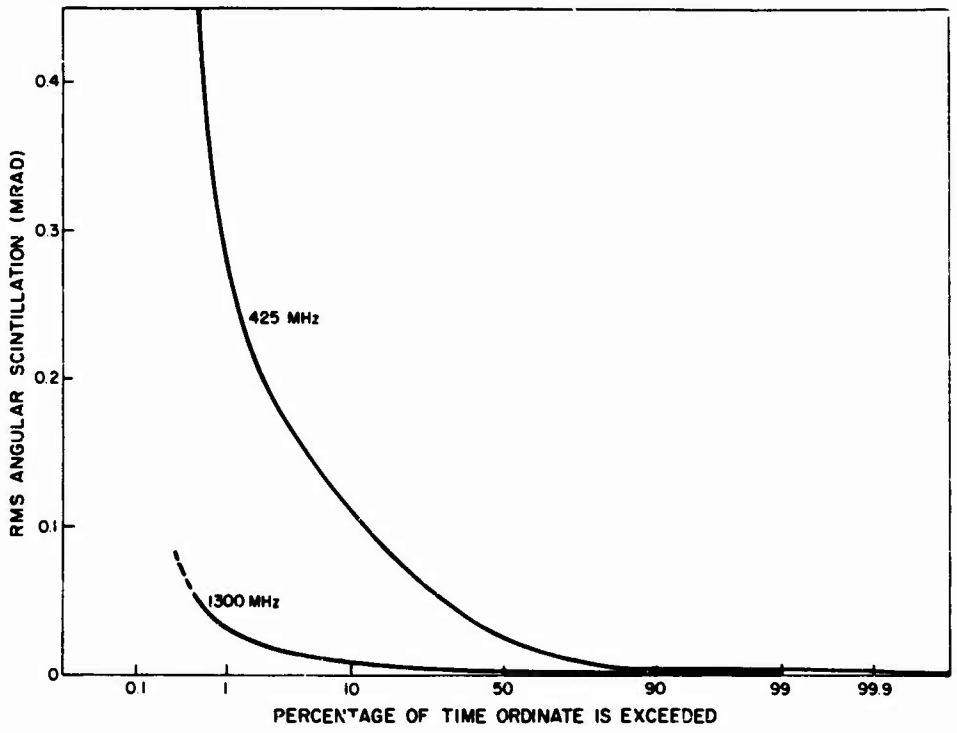


Figure 5.14. Probability Density of Angular Flicker at Fairbanks, Alaska for 425 MHz and 1300 MHz (after Little et al, 1962)

Observations of radio star scintillation from Fairbanks, Alaska (Little et al, 1962) at 223 MHz and 456 MHz may be used to estimate the average probability density of angular flicker for the Clear radar. These estimates, for 425 MHz and 1300 MHz, are displayed in Figure 5.14. The Langmuir probe observations of electron density irregularities reported by Dyson (1969) showed a tendency for the intensity of irregularities to diminish somewhat near the magnetic pole, but the data in this region may be less reliable than for lower latitudes, due to the nature of the satellite orbit. It is probably not too pessimistic to assume values for the irregularity intensity at Thule which are comparable to those at Clear, in order to estimate the magnitude of the angular flicker for that site.

## 5.12 ELEVATION ANGLE DEPENDENCE

Whereas the elevation refraction error increases down to about $5^{o}$ elevation roughly as the secant of the elevation angle, for a spherically stratified ionosphere, the same elevation dependence will not generally be exhibited by the irregular

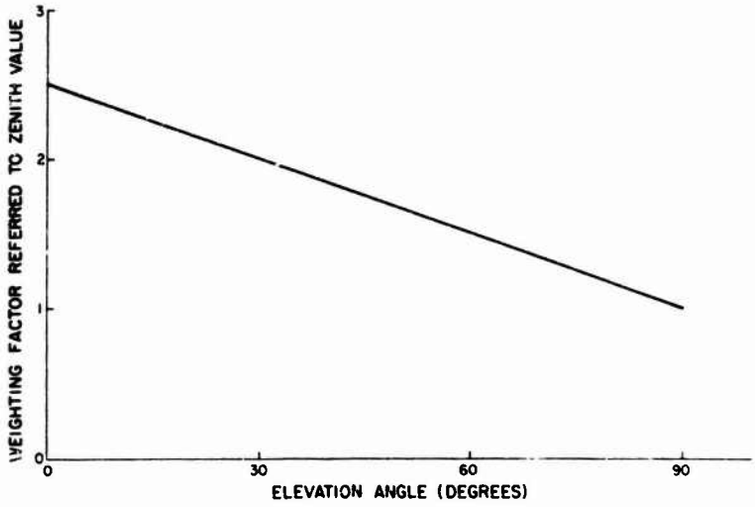


Figure 5.15. Suggested Scaling Law for Converting Irregular Astronomical Refraction at the Zenith to Arbitrary Elevation Angle

refraction component. It was shown by Lawrence et al (1964) that this would in fact be the case for thin prism-like irregularities, but this is not an appropriate model in practice. In fact, the irregularity shape (for large irregularities at least) is more nearly spherical or cylindrical. The irregularities discussed by Titheridge (1968) were found to have a vertical thickness of 0.4 times the horizontal thickness, on the average. Similar ratios were reported by Mirkotan (1960) and Titheridge (1963). Thus the elevation error may vary only by a factor of about 2.5 from zenith to near the horizon. This conclusion has been qualitatively substantiated by some refraction measurements at Sagamore Hill using a satellite near the radio horizon. The amplitude of the irregular refraction component did not greatly exceed the value for a satellite at $39^{o}$ elevation.

Similarly, the magnitude of the small scale fluctuations is observed to increase less slowly towards the horizon than the idealized secant law would predict, assuming uniform irregularity distribution and a plane irregularity layer. Again, a factor of about 2 - 3 would be appropriate for the ratio of small scale angular fluctuation near the horizon to that at the zenith. Figure 5.15 illustrates a suggested approximate scaling law for reducing the values of zenith refraction quoted in this report to arbitrary elevation angles. Due to the highly variable nature of ionospheric irregularity, this should be viewed strictly as an average elevation dependence.

## 5.13 ESTIMATES OF REFRACTION ERRORS

Tables 5.1 and 5.2 contain the best available estimates of the rms errors which might be encountered at the four radar sites, reduced to astronomical refraction at the zenith. Table 5.1 is appropriate for conditions of quiet to moderate geomagnetic and ionospheric activity, while Table 5.2 presents estimates of extreme values which may be infrequently observed (at least at the midlatitude

Table 5.1. Typical RMS Values of Irregular Refraction (mr) for Conditions of Quiet to Moderate Magnetic Activity. Values reduced to astronomical refraction at the zenith.

| Site | Frequency MHz | Large Scale mr | Small Scale mr |
|---|---|---|---|
| Diyarbakir | 425 | 0.005 | 0.003 |
| | 1300 | 0.001 | 0.0003 |
| Shemya | 425 | 0.020 | 0.008 |
| | 1300 | 0.002 | 0.001 |
| Clear | 425 | 0.2 | 0.03 |
| | 1300 | 0.02 | 0.003 |
| Thule | 425 | 0.020 | 0.03 |
| | 1300 | 0.002 | 0.003 |

Table 5.2. Typical RMS Values of Irregular Refraction (mr) for Conditions of Disturbed Magnetic Activity. Values reduced to astronomical refraction at the zenith.

| Site | Frequency MHz | Large Scale mr | Small Scale mr |
|---|---|---|---|
| Diyarbakir | 425 | 0.05 | 0.03 |
| | 1300 | 0.005 | 0.003 |
| Shemya | 425 | 0.2 | 0.05 |
| | 1300 | 0.02 | 0.005 |
| Clear | 425 | 5 | 0.2 |
| | 1300 | 0.5 | 0.02 |
| Thule | 425 | 0.2 | 0.2 |
| | 1300 | 0.02 | 0.02 |

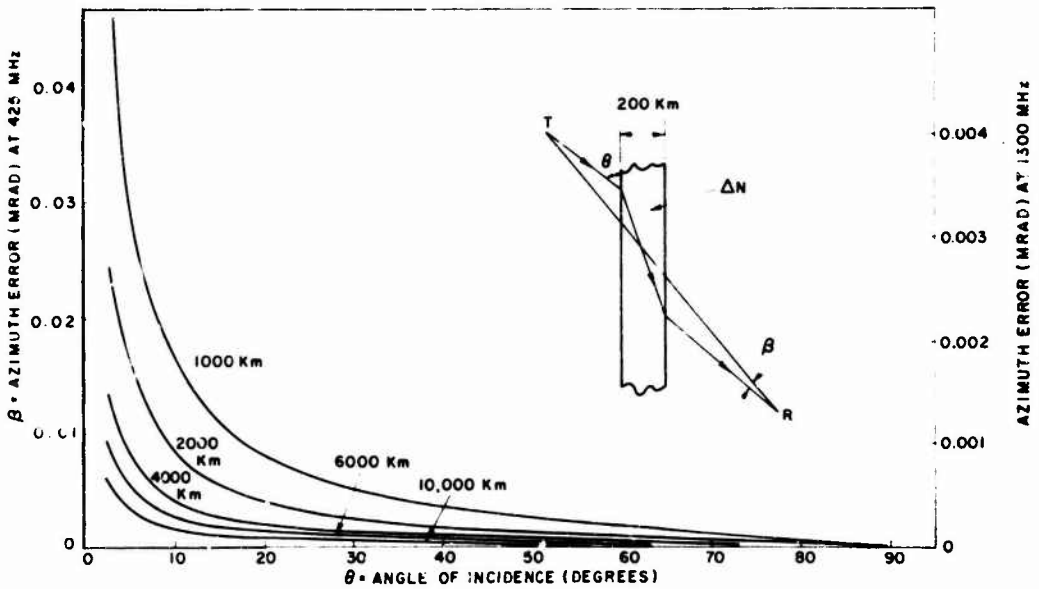


Figure 5.16. Computed Azimuthal Component of Refraction as a Function of Angle of Incidence for Various Target Altitudes for the Model Illustrated of a Slab of Excess Ionization

sites) during conditions of geomagnetic and ionospheric disturbance. These "extreme" values may even be exceeded at the high latitude stations, where the ionospheric variability, as explained previously, is very great. Note particularly that the estimates of large scale refraction in Table 5.2 for Thule, during magnetically disturbed periods, will probably be relevant only when the radar is pointing towards the South near local noon.

### 5.14 AZIMUTH ERRORS

For irregularities having no asymmetry, the refraction errors will be on the average, equally distributed between elevation and azimuth planes. It has been noted, however, that large ionospheric irregularities may be highly asymmetric in projection on the horizontal plane. These irregularities may resemble waves or ripples in the ionosphere, spreading outwards from a localized source of very low-frequency energy. At moderate to large distances from the source, they will appear to an observer as elongated ridges, with the normals to the ridges pointing in the directions shown in Figure 5.3. Under these conditions, the refraction components in the elevation and azimuth planes will be highly dependent upon the orientation of the ridges with respect to the radar beam. In order to illustrate this effect upon the azimuth refraction error, calculations have been performed

using a very simple, highly idealized model. As illustrated in Figure 5.16, this is simply a plane slab of excess ionization embedded in the ionosphere. The angular deviation of the target (T) as viewed by the radar (R) was computed as a function of the angle of incidence, for the radar frequencies. The excess of electron density was chosen as $10^{11}$ $m^{-3}$, the irregularity thickness as 200 km, the irregularity height as 300 km, and the target elevation as $30^{o}$. The computations were performed for various target altitudes as indicated on the curves. Computations were also performed for different thickness and intensity of the irregularity, with the results showing that the azimuth error is fairly closely linearly related to these parameters over a reasonable range.

## References


Bailey, D.K. (1948) Terrest. Magnet. Atm. Elec. 53:41.

Basart, J.P., Miley, G.K. and Clark, B.G. (1970) Trans. IEEE (P.G.A.P.) AP-18:375.

Bhonsle, R.V. (1966) J. Geophys. Res. 71:4571.

Booker, H.G. (1958) Proc. I.R.E. 46:298.

Carru, H., Gendrin, R. and Rayssat, M. (1960) Space Research 1:286.

Dyson, P.L. (1969) J. Geophys. Res. 74:6291.

Fremouw, E.J. (1967) Propagation Factors in Space Communications, AGARD Conference Proceedings No. 3, W.T. Blackband, Ed., (Technavision) p. 225.

Fremous, E.J. and Laksinger, J.A. (1968) J. Geophys. Res. 73:3053.

Getmantsev, G.G. and Eroukhimov, L.M. (1969) Annals of IQSY, Vol. 5, Solar Terrestrial Physics, M.I.T. Press, p. 229.

Hewish, A. (1952) Proc. Ray. Soc. 214:494.

Houminer, Z. (1969) Symposium on the Application of Atmospheric Studies to Satellite Transmissions, Boston (AFCRL).

Jones, J.E. (1969) ESSA Tech Report ERL 142-SDL 11.

Lawrence, R.S., Jespersen, J.L. and Lamb, R.C. (1961) J. Res. (N.B.S.) 65D:333.

Lawrence, R.S., Little, C.G. and Chivers, H.J.A. (1964) Proc. IEEE 52:4.

Little, C.G., Reid, G.C., Stiltner, E. and Merritt, R.P. (1962) J. Geophys. Res. 67:1763.

McIlwain, C.E. (1961) J. Geophys. Res. 66:3681.

Millman, G.H. (1967) Propagation Factors in Space Communications, AGARD Conference Proceedings No. 3, W.T. Blackband, Ed., (Technavision), p. 3.

Mirkotan, S.F. (1960) Issladovaniia neodnorodsostei v. ionosfere, Moscow, Iz. Akad. Nauk. SSSR., 4:20.

Mityakov, N.A., Mityakova, E.E. and Cheropovitskii, V.A. (1968) I.V.U.Z Radiofiz. II, 1324.

## References

Munro, G.H. (1958) Aust. J. Phys. 11:91.

Pfister, W. and Keneshea, T.J. (1956) Air Force Surveys in Geophysics, No. 83, AFCRC TN-56-203.

Smith, F.G. (1952) J. Atmos. Terr. Phys. 2:350.

Stuart, G.F. and Titheridge, J.E. (1969) J. Atmos. Terr. Phys. 31:905.

The Millstone Hill Propagation Study (1969) Tech. Note 1969-51, J.V. Evans, Ed., Lincoln Lab.

Titheridge, J.E. (1963) J. Geophys. Res. 68:3399.

Titheridge, J.E. (1968) J. Atmos. Terr. Phys. 30:73.

Weisbrod, S. and Colin, L. (1960) IRE Trans. Ant. Propagation AP-8:107.